Research Square

Preprints are preliminary reports that have not undergone peer review.
They should not be considered conclusive, used to inform clinical practice,
or referenced by the media as validated information.

Synaptotagmin-7 Deficiency Attenuates Pulmonary Inflammation and Improves Outcomes Following Klebsiella pneumoniae Pneumonia

Madathilparambil V. Suresh
madathil@med.umich.edu
University of Michigan
Vasanth Palanisamy
University of Michigan
Dily Thazhath Sathyarajan
University of Michigan
Leah M Paniker
University of Michigan
Arun Anantharam
University of Toledo
Krishnan Raghavendran
University of Michigan

Research Article

Keywords: Pneumonia, Synaptotagmin-7, Calcium Signaling

Posted Date: November 25th, 2026

DOI: https://doi.org/10.21203/rs.3.rs-11762909/v1

License: This work is licensed under a Creative Commons Attribution 4.0 International License.
Read Full License

Additional Declarations: No competing interests reported.

Synaptotagmin-7 Deficiency Attenuates Pulmonary Inflammation and Improves Outcomes Following Klebsiella pneumoniae Pneumonia

Madathilparambil V. Suresh[1,2], Vasanth Palanisamy[1], Dily Thazhath Sathyarajan[1], Leah M Paniker,[1] Arun Anantharam[3], Krishnan Raghavendran[1]

[1] Department of Surgery, University of Michigan, Ann Arbor, MI, USA
[2] Department of Internal Medicine, Division of Pulmonary and Critical Care Medicine, University of Michigan, Ann Arbor, MI
[3]Department of Neurosciences, University of Toledo, Toledo, OH, USA

Running Title: Syt-7 Regulates Host Defense During Pneumonia

Keywords: Pneumonia; Synaptotagmin-7; Calcium Signaling

*Corresponding author

Madathilparambil V. Suresh
University of Michigan
Ann Arbor, MI 48109, USA
Phone: +1-734-747-2055
Email: madathil@med.umich.edu

Abstract

Synaptotagmin-7 (Syt-7) is a calcium-sensitive protein involved in intracellular membrane trafficking and vesicle fusion. Although Syt-7 plays important roles in cellular secretion and immune cell function, its contribution to host responses during bacterial pneumonia remains poorly understood. This study investigated the role of Syt-7 in pulmonary inflammation and lung injury following *Klebsiella pneumoniae* (KP) infection. Wild-type (WT) and Syt-7-deficient (Syt-7$^{-/-}$) mice were infected intratracheally with a lethal dose of *K. pneumoniae* strain 43816, and survival was monitored for 10 days. At 24 and 48 h after infection, bacterial burdens in the lungs and blood, bronchoalveolar lavage (BAL) cellularity and protein concentrations, pulmonary histopathology, inflammatory mediator levels, inflammatory gene expression, and signaling proteins were assessed. Syt-7$^{-/-}$ mice showed significantly improved survival compared with WT mice, with approximately 70% surviving through day 10, whereas all WT mice died by day 5. Syt-7 deficiency was also associated with reduced bacterial burdens in the lungs and blood, decreased BAL neutrophil accumulation, less severe pulmonary histopathological injury, and lower BAL albumin concentrations. In addition, Syt-7$^{-/-}$ mice exhibited reduced levels of pro-inflammatory cytokines (IL-1β, IL-6, and TNF-α), neutrophil-associated chemokines (KC and MIP-2), and myeloperoxidase. Pulmonary expression of inflammatory genes, including *Il1b*, *Il6*, *Tnf*, *Nos2*, *Arg1*, and *Fizz1*, were also altered in Syt-7-deficient mice. Western blot and qPCR analyses further showed reduced NF-κB p65 protein and *Nlrp3* mRNA expression, respectively. These findings suggest that Syt-7 contributes to pulmonary inflammatory responses and lung injury during *K. pneumoniae* pneumonia. Syt-7 deficiency was associated with improved survival, reduced bacterial burden, and attenuated pulmonary inflammation and lung injury, highlighting Syt-7 as a potential target for further investigation in infection-associated lung injury.

Introduction

Klebsiella pneumoniae (KP) is an encapsulated Gram-negative opportunistic pathogen and a major cause of hospital-acquired infections, including pneumonia and ventilator-associated pneumonia (VAP). Severe KP pneumonia can trigger excessive pulmonary inflammation, tissue injury, and acute respiratory distress syndrome (ARDS), particularly in critically ill and immunocompromised patients. Recent studies have further demonstrated that KP-associated lung injury involves interactions among the pathogen, alveolar macrophages, neutrophils, and the airway epithelium (1, 2). Major trauma and pulmonary contusion are additional risk factors for ARDS. Effective pulmonary host defense therefore requires a coordinated response that promotes bacterial clearance while limiting excessive inflammation and tissue damage.

Synaptotagmins (Syts) are a family of calcium (Ca^{2+})-binding proteins involved in regulated exocytosis and intracellular membrane trafficking. Their conserved C2A and C2B domains mediate calcium sensing and interactions with cellular membranes. Although synaptotagmin-1 (Syt1) and synaptotagmin-2 are best known for their roles in rapid neurotransmitter release, synaptotagmin-7 (Syt-7) has distinct properties, including high calcium sensitivity, that enable it to regulate lysosomal exocytosis, membrane repair, and sustained secretion(3-5). These functions extend the importance of Syt-7 beyond neuronal signaling to cellular processes relevant to innate and adaptive immunity.

Anantharam and colleagues have further investigated Syt-7-dependent calcium sensing and vesicle fusion, showing that Syt-7 enhances the calcium sensitivity of secretory granules and slows the release of granule contents. Related work has also demonstrated that Syt-7 contributes to acetylcholine release during sustained nerve activity, highlighting its role in regulating calcium-dependent secretion (6, 7). Syt-7 also plays an important role in macrophage function and intracellular membrane trafficking. Czibener et al. demonstrated that Syt-7 regulates calcium-dependent lysosomal membrane delivery to nascent phagosomes, supporting efficient phagocytosis, particularly under conditions of high particle burden (8). Syt-7 also regulates lysosomal exocytosis and contributes to plasma membrane repair following cellular injury (4, 9). In cytotoxic T lymphocytes, Syt-7 deficiency impairs cytotoxic effector function and reduces the ability of mice to clear Listeria monocytogenes infection (10). However, subsequent work showed that cytotoxic granule fusion can still occur in the absence of Syt-7, indicating that its contribution to granule exocytosis depends on the experimental conditions (11). Collectively, these findings

suggest that Syt-7 influences multiple cellular processes involved in pathogen handling, membrane trafficking, and immune defense.

Syt-7 has also been implicated in pulmonary inflammation and fibrotic remodeling. Peng et al. demonstrated that Syt-7 promotes macrophage migration and contributes to lung fibrosis in the setting of Plexin C1 deficiency; genetic deletion of Syt-7 attenuated the associated pathological responses (12). More recently, research on intracellular mycobacterial infection has provided further evidence for the role of synaptotagmins in pulmonary immune recognition. A 2023 study demonstrated that endosomal calcium signaling, including Syt-7-dependent trafficking, contributes to MR1-mediated presentation of Mycobacterium tuberculosis antigens (13). In 2026, Kim et al. further demonstrated that Syt1 and Syt-7 promote MR1-dependent activation of mucosal-associated invariant T cells in response to M. tuberculosis-infected cells (14). These findings highlight a role for synaptotagmin-dependent vesicular trafficking in the presentation of intracellular microbial antigens and pulmonary immune responses.

Despite these advances, the role of Syt-7 in antibacterial pulmonary immunity remains incompletely understood. Whether Syt-7 influences bacterial persistence, pulmonary inflammation, or survival following KP infection has not been established. Given its documented roles in macrophage phagocytosis, lysosomal trafficking, and immune-cell function, Syt-7 may influence host responses to bacterial pneumonia through mechanisms that extend beyond its established functions in membrane repair and vesicle fusion.

Building on our previous findings that Toll-like receptor 3 (TLR3) deficiency improves survival, attenuates pulmonary inflammation, and enhances macrophage function during *Klebsiella pneumoniae* (KP) infection (15), and given the limited understanding of synaptotagmin-7 (Syt-7) in pulmonary host defense, we investigated its role in bacterial pneumonia using Syt-7-deficient and wild-type mice. Our findings demonstrate that Syt-7 deficiency is associated with enhanced bacterial clearance, improved survival, and reduced disease severity following KP infection. These findings provide new insights into the contribution of Syt-7 to host defense and pulmonary inflammatory responses during bacterial pneumonia.

Materials and Methods

Animals

All animal procedures were approved by the Institutional Animal Care and Use Committee (IACUC) at the University of Michigan (Protocol No. PRO00011624, “Inflammatory Biology of

Direct Lung Injury") and were conducted in accordance with the Animal Welfare Act, the *Guide for the Care and Use of Laboratory Animals*, NIH guidelines, and applicable state and federal regulations. Age-matched male and female Syt-7-deficient (Syt-$7^{-/-}$) and wild-type (Syt-$7^{+/+}$) mice, 6–8 weeks old, were used, with equal numbers of males and females in each experimental group.

Bacterial pneumonia model

Klebsiella pneumoniae (KP) strain 43816 (serotype 2) was obtained from the American Type Culture Collection (Manassas, VA, USA) and cultured overnight in tryptic soy broth (Becton Dickinson, Franklin Lakes, NJ, USA). Serial dilutions were prepared to achieve a final inoculum of 500 colony-forming units (CFU) in 30 μL. Mice were inoculated with the bacterial suspension or vehicle control by deep oropharyngeal aspiration under isoflurane anesthesia, as previously described (16). Following infection, animals were monitored for 10 days, and health status was assessed every 8 hours according to established criteria (17).

Lungs and blood culture

Bacterial loads in the lungs and blood of KP-infected mice were assessed at 24 and 48 hours. Lungs were aseptically harvested and homogenized in 1 mL of ice-cold phosphate-buffered saline (PBS). A 100 μL aliquot of the homogenate was serially diluted in sterile PBS, plated on 5% sheep blood agar, and incubated overnight at 37 °C. Colony-forming units were then quantified as previously described (17).

Albumin concentrations in bronchoalveolar lavage (BAL)

Albumin concentrations in bronchoalveolar lavage (BAL) fluid were measured using an enzyme-linked immunosorbent assay (ELISA). Briefly, samples were incubated with polyclonal rabbit anti-mouse albumin antibodies to capture albumin present in the BAL fluid. Detection was performed using horseradish peroxidase (HRP)-conjugated goat anti-rabbit IgG secondary antibodies (Bethyl Laboratories, Inc., Montgomery, TX), and signals were developed according to the manufacturer's instructions. Absorbance was measured spectrophotometrically, and albumin concentrations were determined by comparison with a standard curve generated from known concentrations of mouse albumin (18, 19).

Determination of cytokine levels in BAL and lungs:

Soluble levels of IL-1β, IL-4, IL-6, TNF-α, MIP-2, CCL6/MCP-1, CCL12/MCP-5, MPO, IFN-γ, and KC in bronchoalveolar lavage (BAL) fluid and lung tissue following pneumonia were

quantified by ELISA using matched antibody pairs (R&D Systems, Minneapolis, MN) according to the manufacturer's instructions. Cytokine concentrations were determined by comparison with standard curves (20, 21).

Cytospin cell count

Bronchoalveolar lavage (BAL) cells were collected and centrifuged onto glass slides at 600 × g for 5 minutes using a Cytospin II centrifuge (Shandon Scientific, Pittsburgh, PA). Slides were air-dried and stained with Diff-Quik (Dade Behring, Inc., Newark, DE) according to the manufacturer's protocol to differentiate cell types. Stained cells were examined under a light microscope at 20× magnification, and cell populations were quantified based on morphology as previously described. At least three fields per slide were analyzed to ensure representative sampling and accurate cell counts (22, 23).

TaqMan Quantitative Real-Time PCR

Total RNA was isolated from whole lung lysates and reverse-transcribed into cDNA using M-MLV reverse transcriptase (Life Technologies, Grand Island, NY). Gene expression was quantified by real-time TaqMan PCR on an ABI Prism 7700 sequence detection system, with GAPDH used as an internal control. TaqMan gene expression assays and PCR master mix were used to measure inflammation-related transcripts. Relative expression levels were calculated as fold changes compared with controls, as previously described (18, 23).

Histology

Lung tissues were fixed in 10% neutral-buffered formalin, embedded in paraffin, and sectioned at 4–5 μm. Sections were stained with hematoxylin and eosin (H&E) to assess tissue morphology and inflammation. Lung injury in mice was scored using a modification of the ATS lung injury scoring system (Matute-Bello et al., 2011). Alveolar and interstitial neutrophils, hyaline membranes, proteinaceous debris, and alveolar septal thickening were assessed in five randomly selected fields per section at ×20 magnification. All mouse histological scoring was performed by an investigator blinded to genotype and injury condition (22, 24).

Western (WES) Analysis

Protein expression was analyzed using the WES automated capillary Western blot system (ProteinSimple, San Jose, CA, USA) according to the manufacturer's instructions, with a 12–230 kDa separation module (SM-W004) and an anti-rabbit detection module (DM-001). Lung lysates were diluted in 0.1× Sample Buffer (prepared by diluting 10× Sample Buffer 2 1:100), combined

with 5× Fluorescent Master Mix, and denatured at 95°C for 5 min. Each capillary was loaded with 1 µg of total protein. Samples, blocking reagent, primary antibodies diluted in antibody diluent, HRP-conjugated secondary antibody, and chemiluminescent substrate were dispensed into the assay plate. Separation, immunodetection, and chemiluminescent signal acquisition were performed automatically by the instrument. Data was analyzed with Compass for Simple Western software. NF-Kb and NLRP3 peak area were normalized to GAPDH peak area, and apparent molecular weights were determined from the system's internal standards (17, 23).

Statistical methods

Data are presented as mean ± standard error of the mean (SEM). Statistical analyses were performed using GraphPad Prism 11 (La Jolla, CA). Comparisons between groups were performed using one-way analysis of variance (ANOVA) followed by appropriate post hoc analysis, while comparisons between two groups were performed using two-tailed unpaired Student's t-tests with Welch's correction. Survival curves were analyzed using the Kaplan–Meier method and compared using the log-rank test. A p value < 0.05 was considered statistically significant (18, 23, 24).

Results

1. Syt-7 Deficiency Reduces Mortality and Bacterial Burden in Klebsiella pneumoniae–Induced Pneumonia

To determine the role of Syt-7 during bacterial pneumonia, WT and Syt-$7^{-/-}$ mice (n = 10 per group) were challenged intrapharyngeally with a lethal dose of *Klebsiella pneumoniae* (KP), and survival was monitored for 10 days (n=10/group). Syt-$7^{-/-}$ mice showed significantly improved survival compared with WT mice. While all WT mice died by day 5 after infection, approximately 70% of Syt-$7^{-/-}$ mice survived throughout the study period (Figure 1a). These findings suggest that Syt-7 contributes to mortality during KP pneumonia. We next examined bacterial burden in the blood and lungs following infection. Blood samples collected 24 h after infection and cultured on sheep blood agar showed markedly fewer bacterial colonies in Syt-$7^{-/-}$ mice than in WT mice (n = 6/group) (Figure 1b). Consistent with this finding, bacterial counts in lung homogenates were significantly lower in Syt-$7^{-/-}$ mice at both 24 and 48 h post-infection (Figures 1c and 1d). To further confirm the difference in bacterial burden, we measured expression of the *Klebsiella* hemolysin (*khe*) gene in lung tissue. *Khe* expression was significantly reduced in Syt-$7^{-/-}$ mice compared with WT controls (n = 6/group) (Figure 1e). Together, these results show that Syt-7

deficiency is associated with reduced bacterial burden in the lungs and bloodstream during KP pneumonia, which may contribute to the improved survival observed in Syt-7$^{-/-}$ mice.

2. Syt-7 Deficiency Reduces Neutrophil Infiltration and Lung Injury Following *Klebsiella pneumoniae* Infection

We examined inflammatory cell recruitment in WT and Syt-7$^{-/-}$ mice 24 h after *Klebsiella pneumoniae* infection. Total cell counts in bronchoalveolar lavage (BAL) fluid were similar between the two groups (Figure 2a). Differential cell counts showed no significant difference in macrophage numbers (Figure 2b), but neutrophil numbers were significantly lower in Syt-7$^{-/-}$ mice than in WT controls (Figure 2c). We also examined Wright–Giemsa-stained BAL cytospin preparations. Representative images showed fewer inflammatory cells in samples from Syt-7$^{-/-}$ mice (Figure 2d). Consistent with these observations, quantitative analysis showed significantly lower numbers of both macrophages and neutrophils in Syt-7$^{-/-}$ mice (Figure 2e). We next examined lung tissue to assess the extent of injury following infection. We next examined lung histopathology following infection. Representative H&E-stained lung sections from WT mice showed marked inflammatory cell infiltration and disruption of alveolar architecture, whereas lungs from Syt-7$^{-/-}$ mice exhibited substantially less inflammation and preserved lung structure (Figure 2f). Consistent with these observations, lung injury scores were significantly lower in Syt-7$^{-/-}$ mice than in WT controls (n = 3/group) (Figure 2g). Together, these findings demonstrate that Syt-7 deficiency attenuates inflammatory cell recruitment, particularly neutrophil accumulation, and reduces lung injury during *Klebsiella pneumoniae* pneumonia.

3. Syt-7 Deficiency Reduces Lung Injury and Inflammation Following *Klebsiella pneumoniae* Pneumonia

To determine whether Syt-7 contributes to lung injury during KP pneumonia, we measured albumin levels in BAL fluid after infection. Syt-7$^{-/-}$ mice had significantly lower BAL albumin levels than WT mice at both 24 and 48 h post-infection, indicating reduced lung injury (Figure 3a). We next measured inflammatory mediators in BAL fluid. Levels of IL-1β, IL-6, and TNF-α were significantly lower in Syt-7$^{-/-}$ mice than in WT controls following infection (Figures 3b–d). Similarly, the neutrophil-associated chemokines KC and MIP-2 were markedly reduced in Syt-7$^{-/-}$ mice (Figures 3e–f). MPO levels were also significantly lower in Syt-7$^{-/-}$ mice at both points examined (Figure 3g). In addition, MCP-1 and MCP-5 levels were reduced in Syt-7$^{-/-}$ mice,

particularly at 48 h post-infection (n = 10/group) (Figures 3h–i). Together, these results show that loss of Syt-7 reduces lung injury and inflammatory mediator production during KP pneumonia.

4. Syt-7 Deficiency Reduces Pulmonary Inflammatory Gene Expression Following *Klebsiella pneumoniae* Infection

To further assess pulmonary inflammatory responses during KP pneumonia, total RNA was isolated from lung tissue, and gene expression was analyzed by RT-qPCR. Expression of the pro-inflammatory cytokines IL-1β, IL-6, and TNF-α was markedly increased in WT mice following infection but was significantly reduced in Syt-7$^{-/-}$ mice (Figures 4a–c). We next examined the expression of genes associated with macrophage activation and inflammatory responses. NOS2 expression was significantly elevated in WT mice at both 24 and 48 h after infection, whereas Syt-7$^{-/-}$ mice showed substantially lower expression levels (Figure 4d). Similarly, expression of Arginase-1 and FIZZ1 was markedly increased in WT mice following infection but remained significantly lower in Syt-7$^{-/-}$ mice (n = 6/group) (Figures 4e–f). Together, these findings demonstrate that Syt-7 deficiency is associated with reduced expression of inflammatory genes in the lungs during KP pneumonia.

5. Syt-7 Deficiency Reduces NF-κB and NLRP3 Expression Following *Klebsiella pneumoniae* Infection

To investigate the mechanisms underlying the reduced inflammatory response observed in Syt-7$^{-/-}$ mice, we examined expression of NF-κB p65 and NLRP3 in lung tissue following KP infection. NF-κB p65 expression was significantly increased in WT mice after infection but remained markedly reduced in Syt-7$^{-/-}$ mice, as demonstrated by qPCR analysis (Figure 5a). These findings were confirmed by capillary Western blot analysis and electropherogram profiles, which showed substantially lower NF-κB p65 protein expression in Syt-7$^{-/-}$ mice compared with WT controls (n = 6/group) (Figures 5b–c). Similarly, NLRP3 expression was markedly elevated in WT mice following infection but significantly attenuated in Syt-7$^{-/-}$ mice (Figure 5d). Capillary Western blot analysis and electropherogram data further confirmed reduced NLRP3 protein expression in Syt-7$^{-/-}$ mice compared with WT mice (n = 6/group) (Figures 5e–f). Together, these findings indicate that Syt-7 deficiency suppresses activation of the NF-κB/NLRP3 inflammatory signaling pathway during *Klebsiella pneumoniae* pneumonia.

6. Schematic illustration of Syt-7 in Klebsiella pneumoniae pneumonia and its deletion effects.

Schematic illustrating the role of synaptotagmin-7 (Syt-7) in *Klebsiella pneumoniae*–induced pneumonia. Infection activates NF-κB and NLRP3 signaling, driving pro-inflammatory cytokine production, neutrophil infiltration, and lung injury. Syt-7 deletion attenuates these pathways, reduces inflammation, modulates macrophage-associated inflammatory gene expression, enhances bacterial clearance, and improves survival. Overall, this figure summarizes a dual mechanistic effect of Syt-7 deletion: suppression of excessive inflammatory signaling (via NF-κB and NLRP3 pathways) and enhancement of bacterial clearance, leading to improved outcomes in bacterial pneumonia.

Discussion

Bacterial pneumonia remains a major cause of morbidity and mortality, particularly in critically ill patients. Lung contusion (LC) following blunt thoracic trauma increases the risk of acute lung injury (ALI) and acute respiratory distress syndrome (ARDS) (25). *Klebsiella pneumoniae* (KP) is an important cause of severe pneumonia and can induce extensive pulmonary inflammation and systemic infection. We previously showed that direct pulmonary delivery of solubilized curcumin improves survival and reduces bacterial burden and lung injury in a murine model of KP pneumonia(17). In the present study, we investigated the role of synaptotagmin-7 (Syt-7) in host defense against KP infection. Syt-7 deficiency improved survival, reduced bacterial burden in the lungs and bloodstream, decreased pulmonary permeability, and attenuated inflammation. These findings suggest that Syt-7 contributes to disease severity during KP pneumonia.

Syt-7 regulates calcium-dependent membrane trafficking and lysosomal exocytosis. Previous studies have shown that it supports lysosomal membrane delivery to nascent phagosomes during macrophage phagocytosis (8). Syt-7 also regulates macrophage migration and contributes to pulmonary fibrosis in experimental models(12). More recently, Syt-7 was implicated in MR1-mediated presentation of *Mycobacterium tuberculosis* antigens, highlighting its role in intracellular trafficking and pulmonary immune responses (14). Despite these findings, its contribution to KP pneumonia has not been established. In our study, all wild-type (WT) mice succumbed to infection by day 5, whereas approximately 70% of Syt-7-deficient mice survived. This survival benefit was accompanied by reduced bacterial burden and less severe lung injury, suggesting that Syt-7 influences both bacterial control and the inflammatory response to infection.

Excessive inflammation during bacterial pneumonia can disrupt the alveolar-capillary barrier and promote neutrophil recruitment, contributing to pulmonary tissue damage. Consistent with this process, WT mice exhibited greater neutrophil accumulation and more pronounced histological lung injury than Syt-7-deficient mice. Total bronchoalveolar lavage (BAL) cell counts and alveolar macrophage numbers were comparable between groups, suggesting that the differences in inflammation were not simply due to changes in the overall number of recovered cells. The reduced neutrophil accumulation and tissue injury in Syt-7-deficient mice may partly explain their improved outcomes. However, further studies are needed to determine whether Syt-7 directly regulates neutrophil recruitment or activation. Experiments assessing neutrophil chemotaxis, activation markers, and neutrophil depletion or cell-specific Syt-7 deletion could help distinguish direct effects on neutrophils from indirect effects mediated by other cell types.

Macrophages play an essential role in bacterial clearance during pneumonia. We previously demonstrated that TLR3 deficiency improves survival during KP infection by enhancing alveolar macrophage phagocytic and bactericidal activity(15). In the present study, Syt-7 deficiency was associated with lower bacterial burdens and reduced expression of the *Klebsiella* hemolysin (*khe*) gene. Because Syt-7 regulates phagosome formation and lysosomal membrane delivery, altered intracellular trafficking could contribute to the differences in bacterial control. Lysosomal degradation has also been shown to support sustained bacterial uptake by macrophages through a pathway involving NF-κB signaling (26). Nevertheless, the *khe* assay alone does not establish intracellular bacterial viability or directly demonstrate enhanced bacterial killing. Phagocytosis assays, intracellular bacterial survival assays, and measurements of phagosome–lysosome fusion and phagolysosomal acidification are needed to determine whether Syt-7 deficiency directly alters macrophage uptake, intracellular bacterial killing, or phagolysosomal maturation.

We also observed reduced NF-κB and NLRP3 expression in Syt-7-deficient mice following KP infection. NF-κB regulates the expression of inflammatory mediators and can contribute to NLRP3 inflammasome priming, whereas inflammasome activation requires additional signals. The concurrent reduction in these markers was associated with lower inflammatory cytokine production and improved survival. Our previous curcumin study similarly demonstrated reduced NF-κB and NLRP3 expression alongside decreased bacterial burden and lung injury (17). These findings suggest that reduced inflammatory signaling may contribute to

the protective phenotype observed in Syt-7-deficient mice. However, reduced NF-κB and NLRP3 expression alone does not establish reduced pathway activation or demonstrate that either pathway mediates the survival benefit. Measurements of NF-κB p65 phosphorylation and nuclear translocation, caspase-1 activation, and mature IL-1β and IL-18 would help determine whether these pathways are functionally altered. Further experiments using pathway-specific inhibitors or genetic approaches would be needed to establish whether NF-κB or NLRP3 signaling contributes causally to the protective phenotype.

The improved bacterial clearance observed in Syt-7-deficient mice is notable because Syt-7 normally supports several cellular defense processes, including macrophage phagocytosis. Its absence might therefore be expected to impair, rather than improve, bacterial clearance. One possibility is that the effects of Syt-7 depend on the pathogen and the cellular context. Alternatively, changes in inflammatory signaling or intracellular trafficking may indirectly improve bacterial control. These explanations remain hypotheses and require direct testing, including cell-specific Syt-7 deletion or rescue experiments and functional studies of macrophage bacterial killing. Although our results support a role for Syt-7 in the host response to KP infection, the mechanisms underlying this unexpected phenotype remain unresolved.

This study has several limitations. First, global Syt-7 deletion does not distinguish its functions in macrophages, neutrophils, epithelial cells, or other cell populations. Second, the mechanisms responsible for the reduced bacterial burden were not directly established. Third, reduced NF-κB and NLRP3 expressions do not demonstrate that these pathways are required for the protective phenotype. Finally, the findings were obtained in a murine model and require further validation in human disease.

In summary, Syt-7 deficiency improved survival, reduced bacterial burden, decreased pulmonary permeability, and attenuated inflammation during KP pneumonia. These effects were accompanied by reduced neutrophil accumulation and lower NF-κB and NLRP3 expression. Our findings identify Syt-7 as a potential regulator of bacterial control and inflammation-associated lung injury. Further mechanistic studies are needed to determine which cell types and pathways mediate these effects and whether targeting Syt-7 could provide a therapeutic benefit in severe bacterial pneumonia.

Acknowledgments: The authors gratefully acknowledge the support of the National Institutes of Health Grant, R01 GM111305-01 (K.R).

Author Disclosure

MVS contributed to data curation, investigation, project administration, supervision, validation, and visualization, and wrote the original manuscript draft. VP contributed to data curation and reviewed and edited the manuscript. LP reviewed and edited the manuscript. DS contributed to data curation and reviewed and edited the manuscript. LM reviewed and edited the manuscript. AA contributed to supervision and reviewed and edited the manuscript. KR contributed to funding acquisition, resources, supervision, and reviewed and edited the manuscript. All authors reviewed and approved the final manuscript.

Figure legends

Figure 1. Syt-7 deficiency improves survival and reduces bacterial burden during *Klebsiella pneumoniae* infection.

Survival of WT and Syt-7$^{-/-}$ mice was monitored for 10 days following intrapharyngeal challenge with a lethal dose of *K. pneumoniae*, demonstrating significantly improved survival in Syt-7$^{-/-}$ mice (a). Representative blood agar plates and quantification of bacterial burden in blood collected 24 h after infection demonstrated reduced bacteremia in Syt-7$^{-/-}$ mice compared with WT controls (b). Bacterial burden in lung homogenates was significantly lower in Syt-7$^{-/-}$ mice at both 24 h (c) and 48 h (d) post-infection. Consistent with these findings, expression of the *Klebsiella* hemolysin (*khe*) gene was significantly reduced in lung tissue from Syt-7$^{-/-}$ mice 24 h after infection (e). Data are presented as mean ± SEM. $P < 0.05$, $P < 0.01$ versus WT.

Figure 2. Syt-7 deficiency reduces neutrophil recruitment following *Klebsiella pneumoniae* infection. Total bronchoalveolar lavage (BAL) cell counts in WT and Syt-7$^{-/-}$ mice 24 h after infection (a). Differential cell counts showing macrophage and neutrophil numbers, respectively (b, c). Macrophage numbers were similar between groups, whereas neutrophil numbers were significantly lower in Syt-7$^{-/-}$ mice. Representative Wright–Giemsa-stained BAL cytospin images (d). Quantification of macrophage and neutrophil numbers in cytospin preparations (e). Representative H&E-stained lung sections collected 24 h after infection demonstrated reduced inflammatory cell infiltration and preservation of alveolar architecture in Syt-7$^{-/-}$ mice compared with WT mice (f). These histological findings were supported by significantly lower lung injury pathology scores in Syt-7$^{-/-}$ mice (g). Data are presented as mean ± SEM. $P < 0.05$, $P < 0.01$ versus WT.

Figure 3. Syt-7 deficiency attenuates lung injury and inflammatory mediator production following *Klebsiella pneumoniae* infection.

BAL albumin levels were significantly reduced in Syt-7$^{-/-}$ mice at 24 and 48 h post-infection compared with WT mice, indicating decreased alveolar-capillary barrier injury (a). Pro-inflammatory cytokines IL-1β, IL-6, and TNF-α were significantly lower in Syt-7$^{-/-}$ mice than in WT controls (b–d). Similarly, the neutrophil-recruiting chemokines KC and MIP-2, as well as myeloperoxidase (MPO), were markedly reduced in Syt-7$^{-/-}$ mice following infection (e–g). Levels of MCP-1 and MCP-5 were also decreased in Syt-7$^{-/-}$ mice, particularly at 48 h post-infection (h–i). Data are presented as mean ± SEM. $P < 0.05$ versus WT + KP.

Figure 4. Syt-7 deficiency reduces inflammatory gene expression in the lungs following *Klebsiella pneumoniae* infection.

Total RNA was isolated from lung tissue of WT and Syt-7$^{-/-}$ mice following infection, and gene expression was analyzed by RT-qPCR. Syt-7$^{-/-}$ mice exhibited significantly lower expression of the pro-inflammatory cytokines IL-1β, IL-6, and TNF-α compared with WT controls (a–c). Expression of NOS2 was also significantly reduced in Syt-7$^{-/-}$ mice at both 24 and 48 h post-infection (d). Similarly, expression of Arginase-1 and FIZZ1 was markedly lower in Syt-7$^{-/-}$ mice compared with WT mice following infection (e–f). These findings demonstrate that Syt-7 deficiency is associated with reduced pulmonary inflammatory gene expression during *Klebsiella pneumoniae* pneumonia. Data are presented as mean ± SEM. $P < 0.05$ versus WT + KP.

Figure 5. Syt-7 deficiency reduces NF-κB p65 and NLRP3 expression during *Klebsiella pneumoniae* pneumonia.

Lung tissue was collected 24 h after infection and analyzed for NF-κB p65 and NLRP3 expression. qPCR analysis demonstrated significantly lower NF-κB p65 expression in Syt-7$^{-/-}$ mice compared with WT controls (a). Representative capillary Western blot images and electropherogram profiles confirmed reduced NF-κB p65 protein expression in Syt-7$^{-/-}$ mice (b–c). Similarly, NLRP3 mRNA expression was significantly decreased in Syt-7$^{-/-}$ mice following infection (d). Capillary Western blot analysis and electropherogram profiles further demonstrated reduced NLRP3 protein expression in Syt-7$^{-/-}$ mice compared with WT mice (e–f). These findings suggest that Syt-7 contributes to activation of NF-κB/NLRP3 signaling during bacterial pneumonia. Data are presented as mean ± SEM. $P < 0.05$ versus WT + KP.

Figure 6. Proposed mechanism underlying protection in Syt-7$^{-/-}$ mice during *Klebsiella pneumoniae* pneumonia.

Following intrapharyngeal *Klebsiella pneumoniae* infection, WT mice exhibit enhanced activation of NF-κB p65 signaling, leading to increased NLRP3 inflammasome expression and elevated production of pro-inflammatory cytokines (IL-1β, IL-6, TNF-α) and chemokines (KC/CXCL1, MIP-2/CXCL2). This heightened inflammatory response is associated with increased neutrophil recruitment, greater bacterial burden, enhanced lung permeability (BAL albumin), and increased lung injury, resulting in poor survival outcomes. In contrast, Syt-7 deficiency suppresses NF-κB p65 activation and NLRP3 expression, leading to reduced cytokine and chemokine production, decreased neutrophilic inflammation, lower bacterial burden, and attenuated lung injury. Collectively, these effects promote improved bacterial clearance, reduced pulmonary inflammation, and enhanced survival in Syt-7$^{-/-}$ mice following *K. pneumoniae* infection. The schematic summarizes the proposed role of Syt-7 as a positive regulator of NF-κB/NLRP3-mediated inflammatory signaling during bacterial pneumonia.

References

1. Cui J, Xu Z, Yu Z, Zhang Q, Liu S, Du B, et al. High-alcohol-producing Klebsiella pneumoniae aggravates lung injury by affecting neutrophils and the airway epithelium. *Cell Rep Med.* 2025;6(1):101886.
2. Xu Q, Liu X, Heng H, Wang H, Zhao W, Luo M, et al. Cytokine-driven PANoptosis of alveolar macrophages mediated by STAT1 underlies acute lung injury in hypervirulent Klebsiella pneumoniae infection. *mBio.* 2026;17(5):e0395825.
3. Martinez I, Chakrabarti S, Hellevik T, Morehead J, Fowler K, and Andrews NW. Synaptotagmin VII regulates Ca(2+)-dependent exocytosis of lysosomes in fibroblasts. *J Cell Biol.* 2000;148(6):1141-49.
4. Reddy A, Caler EV, and Andrews NW. Plasma membrane repair is mediated by Ca(2+)-regulated exocytosis of lysosomes. *Cell.* 2001;106(2):157-69.
5. Jaiswal JK, Chakrabarti S, Andrews NW, and Simon SM. Synaptotagmin VII restricts fusion pore expansion during lysosomal exocytosis. *PLoS Biol.* 2004;2(8):E233.
6. Rao TC, Passmore DR, Peleman AR, Das M, Chapman ER, and Anantharam A. Distinct fusion properties of synaptotagmin-1 and synaptotagmin-7 bearing dense core granules. *Mol Biol Cell.* 2014;25(16):2416-27.
7. Bendahmane M, Morales A, Kreutzberger AJB, Schenk NA, Mohan R, Bakshi S, et al. Synaptotagmin-7 enhances calcium-sensing of chromaffin cell granules and slows discharge of granule cargos. *J Neurochem.* 2020;154(6):598-617.
8. Czibener C, Sherer NM, Becker SM, Pypaert M, Hui E, Chapman ER, et al. Ca2+ and synaptotagmin VII-dependent delivery of lysosomal membrane to nascent phagosomes. *J Cell Biol.* 2006;174(7):997-1007.

9. Rao SK, Huynh C, Proux-Gillardeaux V, Galli T, and Andrews NW. Identification of SNAREs involved in synaptotagmin VII-regulated lysosomal exocytosis. *J Biol Chem.* 2004;279(19):20471-9.
10. Fowler KT, Andrews NW, and Huleatt JW. Expression and function of synaptotagmin VII in CTLs. *J Immunol.* 2007;178(3):1498-504.
11. Sleiman M, Stevens DR, Chitirala P, and Rettig J. Cytotoxic Granule Trafficking and Fusion in Synaptotagmin7-Deficient Cytotoxic T Lymphocytes. *Front Immunol.* 2020;11:1080.
12. Peng X, Moore M, Mathur A, Zhou Y, Sun H, Gan Y, et al. Plexin C1 deficiency permits synaptotagmin 7-mediated macrophage migration and enhances mammalian lung fibrosis. *FASEB J.* 2016;30(12):4056-70.
13. Karamooz E, Peterson J, Tammen A, Soma S, Kim SJ, and Lewinsohn D. Calcium Signaling in MR1-Dependent Antigen Presentation of Mycobacterium tuberculosis. *Res Sq.* 2023.
14. Kim SJ, Peterson JC, Olive AJ, Tafesse FG, Kulicke CA, Karamooz E, et al. Synaptotagmin 1 and Synaptotagmin 7 promote MR1-mediated presentation of Mycobacterium tuberculosis antigens. *Elife.* 2026;14.
15. Suresh MV, Dolgachev VA, Zhang B, Balijepalli S, Swamy S, Mooliyil J, et al. TLR3 absence confers increased survival with improved macrophage activity against pneumonia. *JCI Insight.* 2019;4(23).
16. Dolgachev V, Panicker S, Balijepalli S, McCandless LK, Yin Y, Swamy S, et al. Electroporation-mediated delivery of FER gene enhances innate immune response and improves survival in a murine model of pneumonia. *Gene Ther.* 2018;25(5):359-75.
17. Zhang B, Swamy S, Balijepalli S, Panicker S, Mooliyil J, Sherman MA, et al. Direct pulmonary delivery of solubilized curcumin reduces severity of lethal pneumonia. *FASEB J.* 2019:fj201901047RR.
18. Suresh MV, Ramakrishnan SK, Thomas B, Machado-Aranda D, Bi Y, Talarico N, et al. Activation of hypoxia-inducible factor-1alpha in type 2 alveolar epithelial cell is a major driver of acute inflammation following lung contusion. *Crit Care Med.* 2014;42(10):e642-53.
19. Suresh MV, Yu B, Lakshminrusimha S, Machado-Aranda D, Talarico N, Zeng L, et al. The protective role of MnTBAP in oxidant-mediated injury and inflammation in a rat model of lung contusion. *Surgery.* 2013;154(5):980-90.
20. Suresh MV, Balijepalli S, Zhang B, Singh VV, Swamy S, Panicker S, et al. Hypoxia-Inducible Factor (HIF)-1alpha Promotes Inflammation and Injury Following Aspiration-Induced Lung Injury in Mice. *Shock.* 2018.
21. Suresh MV, Thomas B, Dolgachev VA, Sherman MA, Goldberg R, Johnson M, et al. Toll-Like Receptor-9 (TLR9) is Requisite for Acute Inflammatory Response and Injury Following Lung Contusion. *Shock.* 2016;46(4):412-9.
22. Suresh MV, Yu B, Machado-Aranda D, Bender MD, Ochoa-Frongia L, Helinski JD, et al. Role of macrophage chemoattractant protein-1 in acute inflammation after lung contusion. *Am J Respir Cell Mol Biol.* 2012;46(6):797-806.
23. Suresh MV, Thomas B, Machado-Aranda D, Dolgachev VA, Kumar Ramakrishnan S, Talarico N, et al. Double-Stranded RNA Interacts With Toll-Like Receptor 3 in Driving the Acute Inflammatory Response Following Lung Contusion. *Crit Care Med.* 2016;44(11):e1054-e66.

24. Suresh MV, Wagner MC, Rosania GR, Stringer KA, Min KA, Risler L, et al. Pulmonary administration of a water-soluble curcumin complex reduces severity of acute lung injury. *Am J Respir Cell Mol Biol.* 2012;47(3):280-7.
25. Tignanelli CJ, Hemmila MR, Rogers MAM, and Raghavendran K. Nationwide cohort study of independent risk factors for acute respiratory distress syndrome after trauma. *Trauma Surg Acute Care Open.* 2019;4(1):e000249.
26. Wong CO, Gregory S, Hu H, Chao Y, Sepulveda VE, He Y, et al. Lysosomal Degradation Is Required for Sustained Phagocytosis of Bacteria by Macrophages. *Cell Host Microbe.* 2017;21(6):719-30 e6.

Figure 1

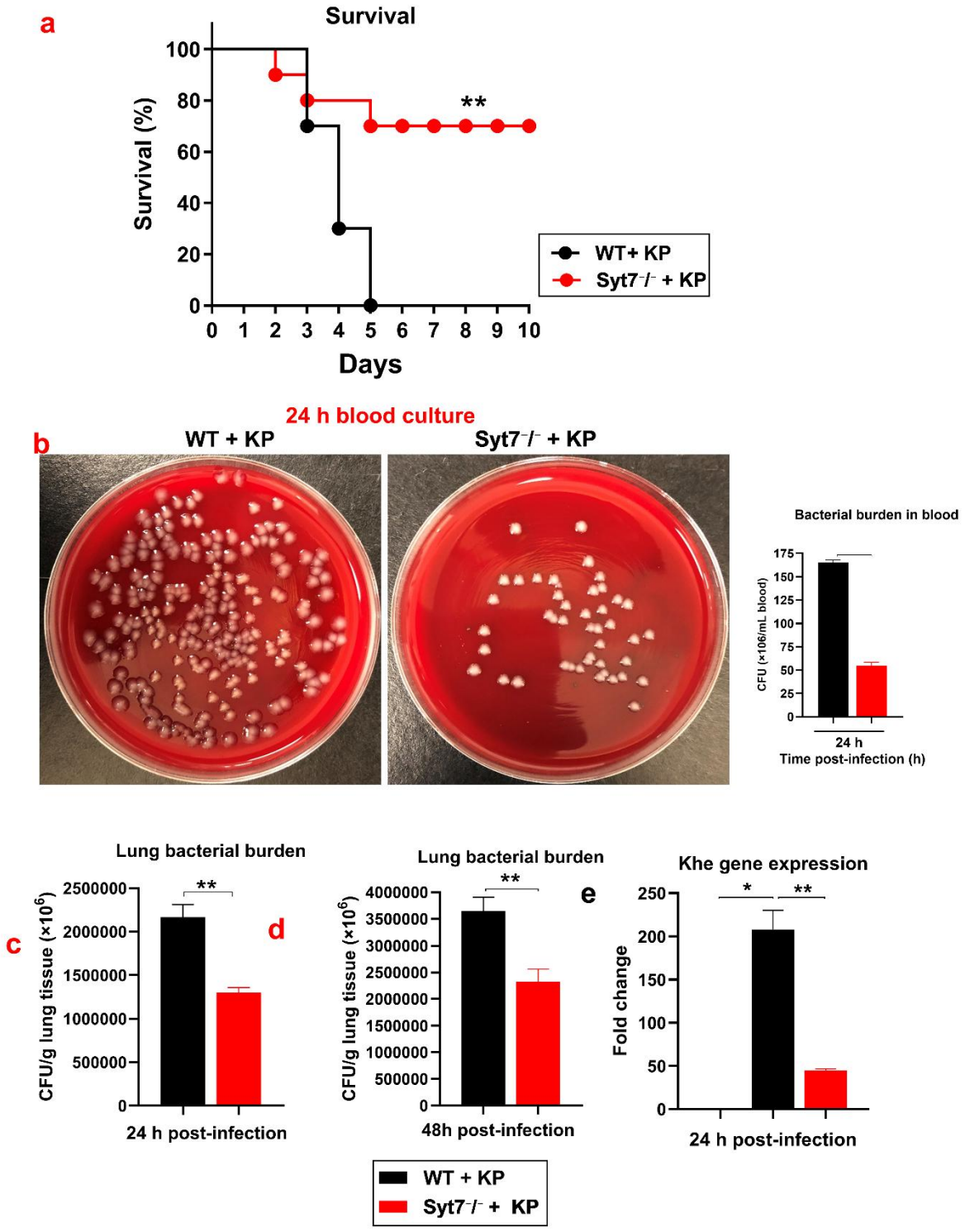

a
Survival
Survival (%)
Days
**
WT+ KP
Syt7-/- + KP
b
24 h blood culture
WT + KP
Syt7-/- + KP
Bacterial burden in blood
CFU (×106/mL blood)
24 h
Time post-infection (h)
c
Lung bacterial burden
CFU/g lung tissue (×10^6)
24 h post-infection
d
Lung bacterial burden
CFU/g lung tissue (×10^6)
48h post-infection
e
Khe gene expression
Fold change
24 h post-infection
WT + KP
Syt7-/- + KP

Figure 2

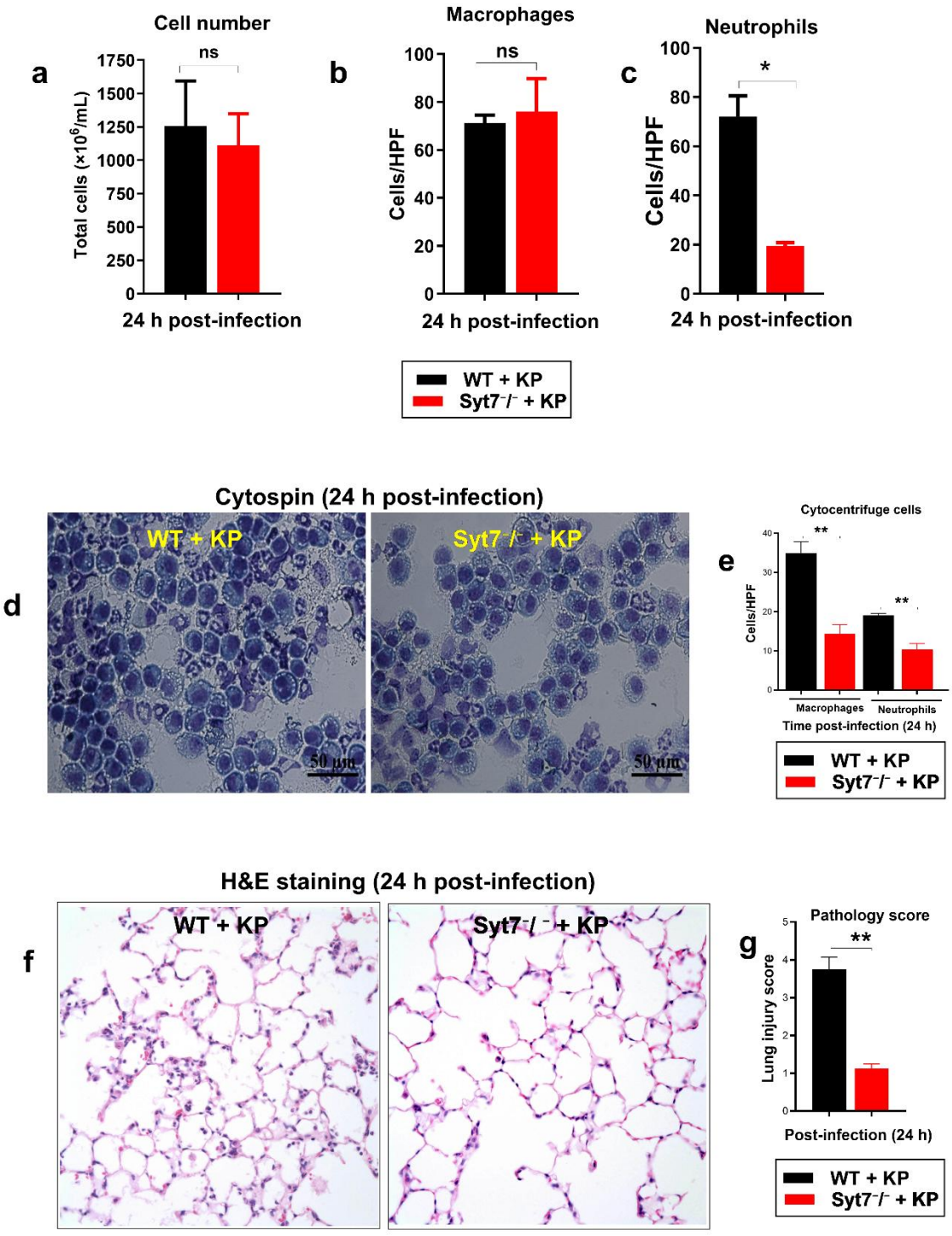

a
Cell number
ns
Total cells (×10^6/mL)
1750
1500
1250
1000
750
500
250
0
24 h post-infection
b
Macrophages
ns
Cells/HPF
100
80
60
40
20
0
24 h post-infection
c
Neutrophils
*
Cells/HPF
100
80
60
40
20
0
24 h post-infection
WT + KP
Syt7-/- + KP
d
Cytospin (24 h post-infection)
WT + KP
Syt7-/- + KP
50 μm
50 μm
e
Cytocentrifuge cells
**
**
Cells/HPF
40
30
20
10
0
Macrophages
Neutrophils
Time post-infection (24 h)
WT + KP
Syt7-/- + KP
f
H&E staining (24 h post-infection)
WT + KP
Syt7-/- + KP
g
Pathology score
**
Lung injury score
5
4
3
2
1
0
Post-infection (24 h)
WT + KP
Syt7-/- + KP

Figure 3

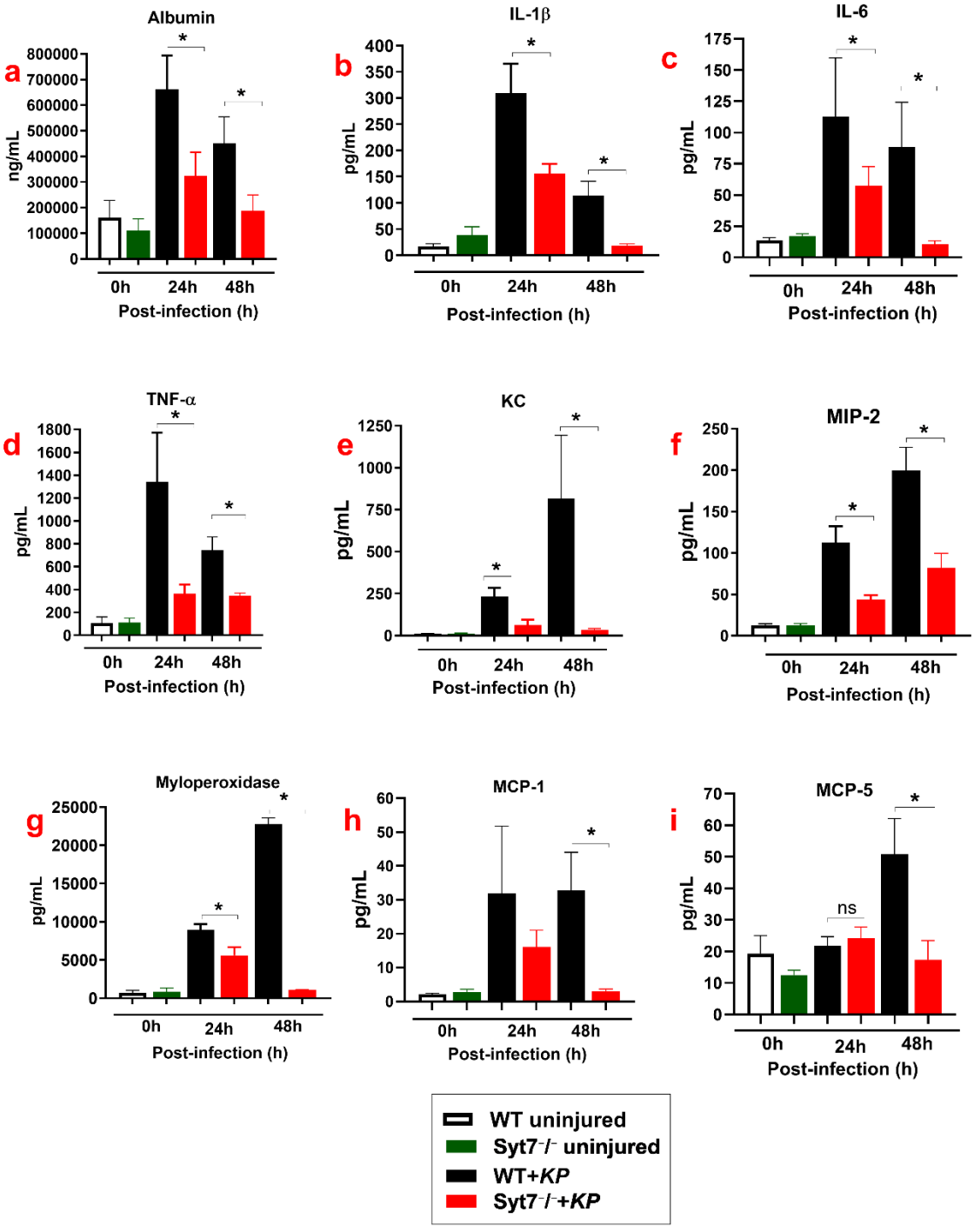

a
Albumin
ng/mL
800000
700000
600000
500000
400000
300000
200000
100000
0
0h
24h
48h
Post-infection (h)
b
IL-1β
pg/mL
400
350
300
250
200
150
100
50
0
c
IL-6
175
150
125
100
75
50
25
d
TNF-α
1800
1600
1400
1200
1000
800
600
400
200
e
KC
1250
1000
750
500
250
f
MIP-2
g
Myloperoxidase
25000
20000
15000
10000
5000
h
MCP-1
i
MCP-5
ns
WT uninjured
Syt7-/- uninjured
WT+KP
Syt7-/-+KP

Figure 4

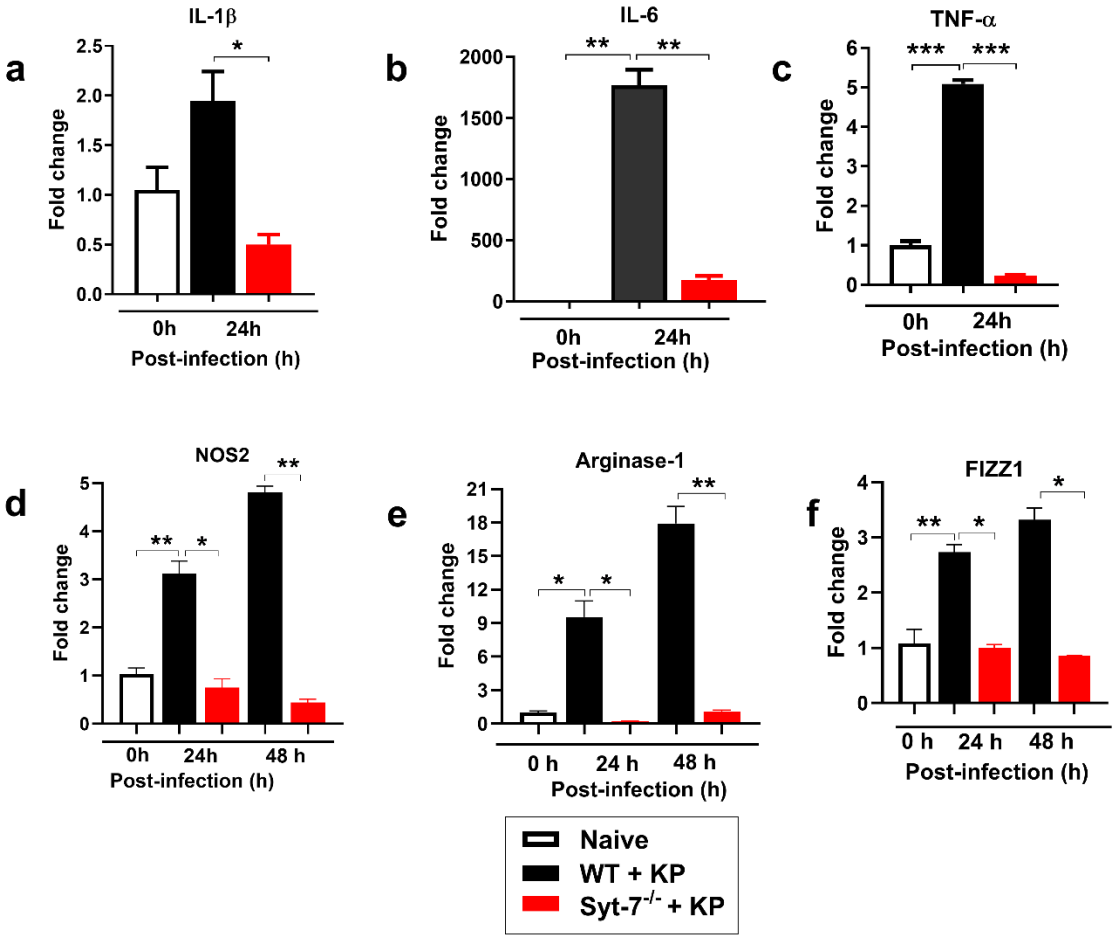

a
IL-1β
Fold change
2.5
2.0
1.5
1.0
0.5
0.0
*
0h
24h
Post-infection (h)
b
IL-6
Fold change
2000
1500
1000
500
0
**
**
0h
24h
Post-infection (h)
c
TNF-α
Fold change
6
5
4
3
2
1
0
***
***
0h
24h
Post-infection (h)
d
NOS2
Fold change
5
4
3
2
1
0
**
*
**
0h
24h
48 h
Post-infection (h)
e
Arginase-1
Fold change
21
18
15
12
9
6
3
0
*
*
**
0 h
24 h
48 h
Post-infection (h)
f
FIZZ1
Fold change
4
3
2
1
0
**
*
*
0 h
24 h
48 h
Post-infection (h)
Naive
WT + KP
Syt-7-/- + KP

Figure 5

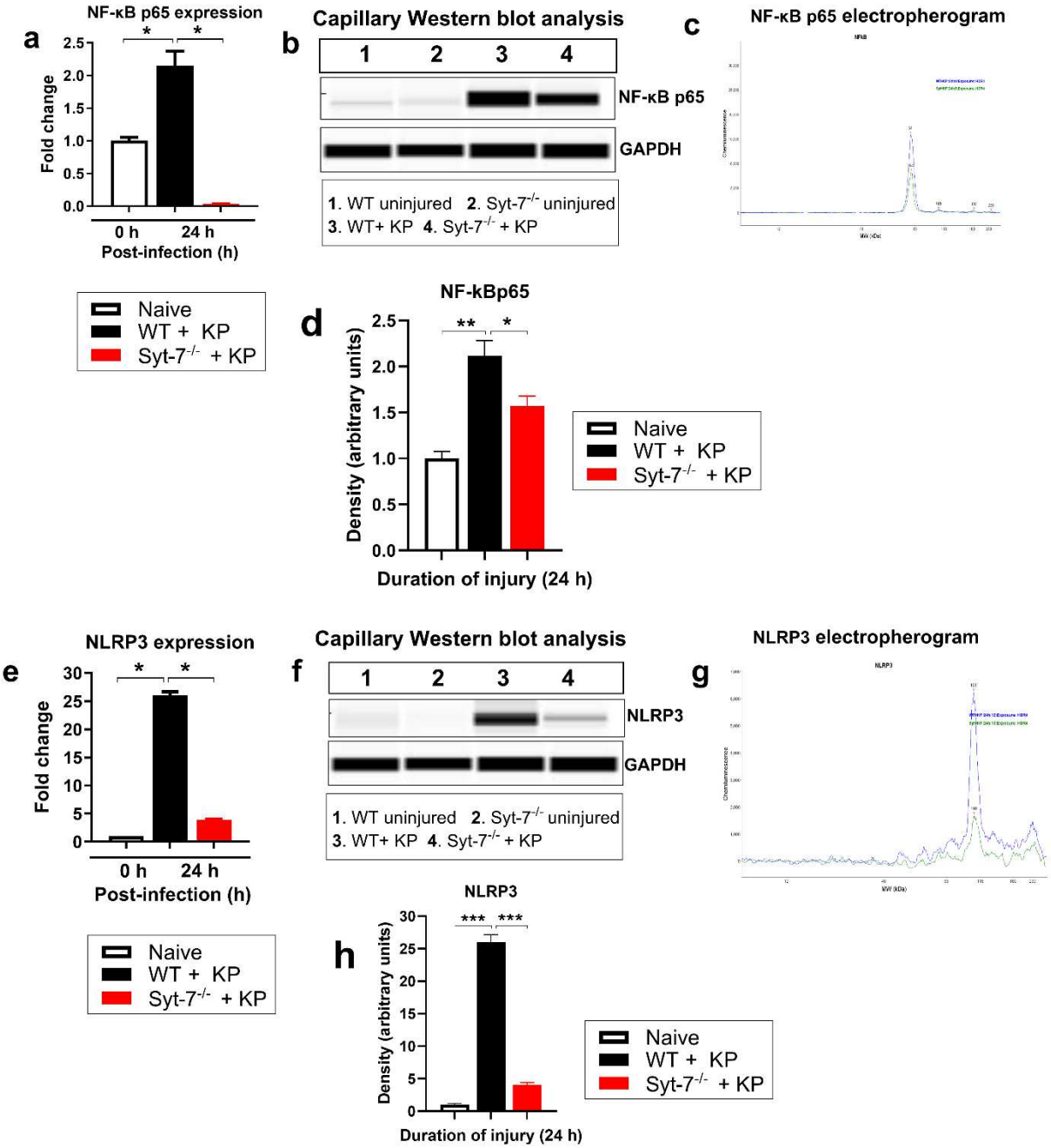
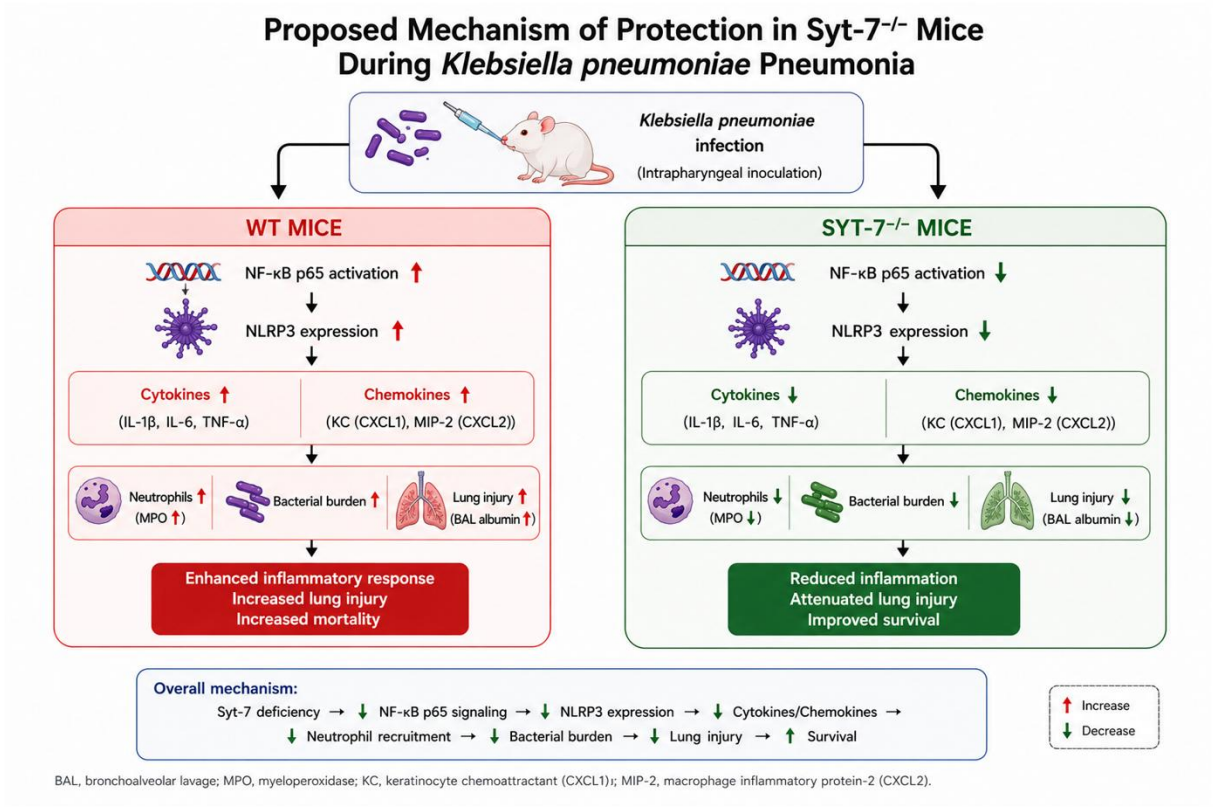

a
NF-κB p65 expression
Fold change
0 h
24 h
Post-infection (h)
Naive
WT + KP
Syt-7-/- + KP
b
Capillary Western blot analysis
1 2 3 4
NF-κB p65
GAPDH
1. WT uninjured 2. Syt-7-/- uninjured
3. WT+ KP 4. Syt-7-/- + KP
c
NF-κB p65 electropherogram
d
NF-kBp65
Density (arbitrary units)
Duration of injury (24 h)
e
NLRP3 expression
f
Capillary Western blot analysis
NLRP3
GAPDH
g
NLRP3 electropherogram
h
NLRP3

Figure 6



BAL, bronchoalveolar lavage; MPO, myeloperoxidase; KC, keratinocyte chemoattractant (CXCL1)ı; MIP-2, macrophage inflammatory protein-2 (CXCL2).